

## Polar head groups are important for barrier-protective effects of oxidized phospholipids on pulmonary endothelium

Anna A. Birukova,<sup>1</sup> Panfeng Fu,<sup>1</sup> Santipongse Chatchavalvanich,<sup>1</sup> Dylan Burdette,<sup>1</sup>  
Olga Oskolkova,<sup>2</sup> Valery N. Bochkov,<sup>2</sup> and Konstantin G. Birukov<sup>1</sup>

<sup>1</sup>Section of Pulmonary and Critical Care Medicine, Department of Medicine, University of Chicago, Chicago, Illinois; and <sup>2</sup>Department of Vascular Biology and Thrombosis Research, University of Vienna, Vienna, Austria

Submitted 5 October 2006; accepted in final form 6 December 2006

**Birukova AA, Fu P, Chatchavalvanich S, Burdette D, Oskolkova O, Bochkov VN, Birukov KG.** Polar head groups are important for barrier-protective effects of oxidized phospholipids on pulmonary endothelium. *Am J Physiol Lung Cell Mol Physiol* 292: L924–L935, 2007. First published December 8, 2006; doi:10.1152/ajplung.00395.2006.—We have previously described protective effects of oxidized 1-palmitoyl-2-arachidonoyl-*sn*-glycero-3-phosphocholine (OxPAPC) on pulmonary endothelial cell (EC) barrier function and demonstrated the critical role of cyclopentenone-containing modifications of arachidonoyl moiety in OxPAPC protective effects. In this study we used oxidized phosphocholine (OxPAPC), phosphoserine (OxPAPS), and glycerophosphate (OxPAPA) to investigate the role of polar head groups in EC barrier-protective responses to oxidized phospholipids (OxPLs). OxPAPC and OxPAPS induced sustained barrier enhancement in pulmonary EC, whereas OxPAPA caused a transient protective response as judged by measurements of transendothelial electrical resistance (TER). Non-OxPLs showed no effects on TER levels. All three OxPLs caused enhancement of peripheral EC actin cytoskeleton. OxPAPC and OxPAPS completely abolished LPS-induced EC hyperpermeability *in vitro*, whereas OxPAPA showed only a partial protective effect. *In vivo*, intravenous injection of OxPAPS or OxPAPC (1.5 mg/kg) markedly attenuated increases in the protein content, cell counts, and myeloperoxidase activities detected in bronchoalveolar lavage fluid upon intratracheal LPS instillation in mice, although OxPAPC showed less potency. All three OxPLs partially attenuated EC barrier dysfunction induced by IL-6 and thrombin. Their protective effects against thrombin-induced EC barrier dysfunction were linked to the attenuation of the thrombin-induced Rho pathway of EC hyperpermeability and stimulation of Rac-mediated mechanisms of EC barrier recovery. These results demonstrate for the first time the essential role of polar OxPL groups in blunting the LPS-induced EC dysfunction *in vitro* and *in vivo* and suggest the mechanism of agonist-induced hyperpermeability attenuation by OxPLs via reduction of Rho and stimulation of Rac signaling.

permeability; lung endothelium; thrombin; lipopolysaccharide; interleukin-6; small guanosine triphosphatases; cytoskeleton; adherens junctions; animals; acute lung injury

THE LUNG ENDOTHELIUM forms a semiselective barrier between circulating blood and interstitial fluid that is dynamically regulated by a counterbalance of barrier-protective and barrier-disruptive bioactive molecules present in the circulation. Accumulating evidence suggests that products of phospholipid oxidation may be involved in innate immunity, chronic inflammation, and vascular barrier regulation (1, 11, 12, 27). Enhanced lipid peroxidation leading to formation of oxidized

phospholipids (OxPLs) has been observed in acute lung injury (ALI) syndromes such as acute respiratory distress syndrome (ARDS), ventilator-induced lung injury, and asthma (14, 48). An increased release of membrane vesicles containing OxPLs has been detected as a result of tissue injury and apoptosis (23, 24). Phosphatidylcholines and phosphatidylserines represent major groups of cell membrane structural phospholipids, and they may become readily oxidized in these pathological processes.

We have previously described potent barrier-protective effects of oxidized 1-palmitoyl-2-arachidonoyl-*sn*-glycero-3-phosphocholine (OxPAPC) on the pulmonary endothelial cells (EC) and identified the critical role of cyclopentenone-containing oxidized modifications of arachidonoyl moiety in the mediation of the OxPAPC effects. In contrast, fragmented products of PAPC oxidation exhibited barrier-disruptive effects (2). Barrier-protective effects of OxPAPC were accompanied by enhancement of peripheral F-actin cytoskeleton and mediated by the small GTPases Rac and Cdc42 (2). OxPAPC also attenuated thrombin-induced EC barrier dysfunction and accelerated recovery of EC monolayer integrity after thrombin challenge (2). However, signaling mechanisms of this protective effect by OxPAPC have not been explored.

Independently of the effects on Rac/Cdc42-mediated F-actin remodeling and enhancement of EC barrier, OxPAPC attenuates inflammatory cascade induced by bacterial lipopolysaccharide (LPS) via antagonistic interaction with the LPS coreceptors LPS-binding protein (LBP) and CD14, which competitively blocks the ability of LPS to bind Toll-like receptor-4 (TLR-4) (10) and blunts the NF- $\kappa$ B-mediated expression of inflammatory cytokines (31). We have shown previously that OxPAPC, but not nonoxidized PAPC, markedly attenuates LPS-induced lung tissue inflammation, barrier disruption, and production of inflammatory cytokines IL-6 and IL-1 $\beta$  over a range of doses in the rat model of LPS-induced lung injury (35). However, effects of other OxPLs on LPS-induced lung injury have not yet been explored. IL-6 itself is a recognized inflammatory cytokine. When bound to a soluble coreceptor, IL-6 activates membrane-bound IL-6 receptor distinct from the TLR family receptors (26). Activation of IL-6 receptor stimulates several pathways, including MAP kinase, phosphatidylinositol 3-kinase (PI3-kinase), and JAK-STAT pathways, and further propagates inflammatory cascade and endothelial barrier dysfunction via activation of expression

Address for reprint requests and other correspondence: K. Birukov, Section of Pulmonary and Critical Care Medicine, Dept. of Medicine, Division of Biomedical Sciences, Univ. of Chicago, 929 East 57th St., CIS Bldg., W410, Chicago, IL 60637 (e-mail: kbirukov@medicine.bsd.uchicago.edu).

The costs of publication of this article were defrayed in part by the payment of page charges. The article must therefore be hereby marked "advertisement" in accordance with 18 U.S.C. Section 1734 solely to indicate this fact.

of inflammatory chemokines CXCL5, CXCL6, CCL2, and CCL8 (26).

In this study, we tested direct effects of OxPLs containing positively charged (oxidized phosphocholine, OxPAPC) and negatively charged (oxidized phosphoserine, OxPAPS) polar head groups as well as oxidized glycerophosphate (OxPAPA), lacking the head group, on the pulmonary endothelial barrier properties and cytoskeletal arrangement and explored the effects of OxPLs on the endothelial barrier dysfunction induced by edemagenic (thrombin) and inflammatory (LPS and IL-6) mediators. Finally, the effects of OxPAPC and OxPAPS were tested in the murine model of ALI.

MATERIALS AND METHODS

**Reagents and cell culture.** Primary antibodies to  $\beta$ -catenin were purchased from BD Transduction Laboratories (San Diego, CA). Human IL-6 and human IL-6 soluble receptor were obtained from R&D Systems (Minneapolis, MN). Texas red-phalloidin and Alexa Flour 488-conjugated secondary antibodies were purchased from Molecular Probes (Eugene, OR). Unless otherwise specified, biochemical reagents were obtained from Sigma (St. Louis, MO). Human pulmonary artery endothelial cells (HPAEC) were obtained from Cambrex (Walkersville, MD), cultured according to the manufacturer's protocol, and used at passages 5–9.

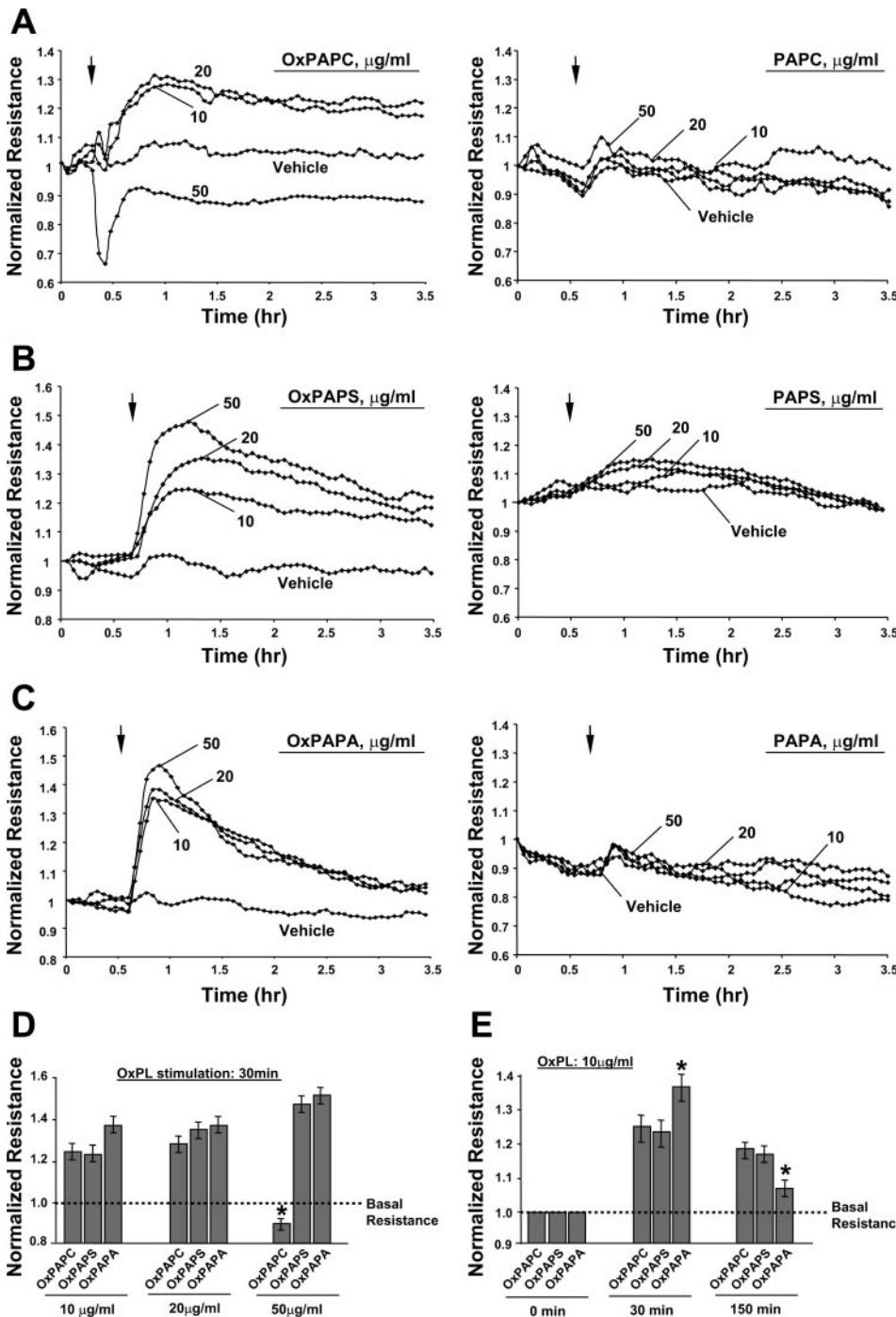


Fig. 1. Effect of oxidized phospholipids (OxPLs) and their nonoxidized forms on endothelial cell (EC) barrier function. A–C: human pulmonary arterial endothelial cell (HPAEC) monolayers were grown on gold microelectrodes. At the time point indicated by the arrow, cells were treated with 10, 20, or 50  $\mu\text{g/ml}$  oxidized phosphocholine (OxPAPC; A, left), phosphoserine (OxPAPS; B, left), or glycerophosphate (OxPAPA; C, left) or their nonoxidized forms (A–C, right), and transendothelial electrical resistance (TER) was monitored for 3.5 h. D: summary of dose-dependent OxPL effects on EC permeability. TER measurements were made after 30 min of EC stimulation with OxPAPC, OxPAPS, or OxPAPA at 10, 20, or 50  $\mu\text{g/ml}$ . E: summary of time-dependent effects of OxPLs on EC permeability. TER was measured after 30 and 150 min of EC treatment with OxPAPC, OxPAPS, or OxPAPA (10  $\mu\text{g/ml}$ ). Results are pooled from 3–8 independent experiments. Data are represented as means (SD).

Downloaded from [ajplung.physiology.org](http://ajplung.physiology.org) on August 22, 2007

**Lipid oxidation and analysis.** 1-Palmitoyl-2-arachidonoyl-*sn*-glycero-3-phosphocholine (PAPC), 1-palmitoyl-2-arachidonoyl-*sn*-glycero-3-[phospho-L-serine] (PAPS), and 1-palmitoyl-2-arachidonoyl-*sn*-glycero-3-phosphate (phosphatidic acid, PAPA) were obtained from Avanti Polar Lipids (Alabaster, AL). Phospholipids were oxidized by exposure of dry lipid to air as previously described (2, 46, 47). The extent of oxidation was measured by positive ion electrospray-mass spectrometry as previously described by our groups (2, 46). OxPAPC preparations contained a characteristic pattern of products with fragmented ( $m/z < 782.7$ ) and oxygenated ( $m/z > 782.7$ ) *sn*-2 residues. Among oxygenated derivatives of PAPC, PEIPC ( $m/z$  828) and PECPC ( $m/z$  810) representing major peaks have been structurally identified and shown to exert biological activities (2, 28, 46). Homologous peaks were present in oxidized PAPS and PAPA preparations. Next, oxidized lipids dissolved in chloroform were stored at  $-80^{\circ}\text{C}$  and used within 2 wk after mass spectrometry testing. All oxidized and nonoxidized phospholipid preparations were analyzed using the limulus amoebocyte assay (BioWhittaker, Frederick, MD) and shown to be negative for endotoxin.

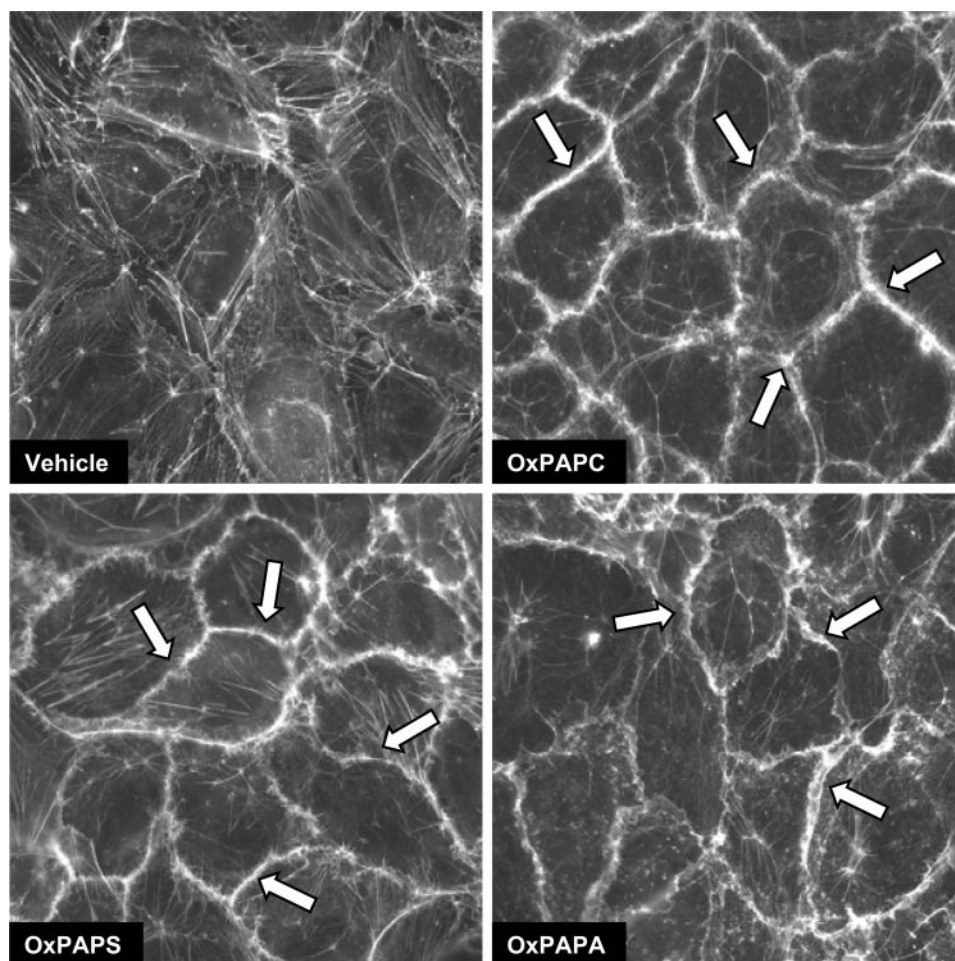
**Measurement of transendothelial electrical resistance.** The cellular barrier properties were analyzed by measurements of transendothelial electrical resistance (TER) across confluent human pulmonary artery endothelial monolayers, using the electrical cell-substrate impedance sensing system (Applied Biophysics, Troy, NY) as previously described (2, 4–6, 9). TER values from at least six microelectrodes corresponding to each experimental condition were pooled at discrete time points with the use of custom-designed Epool software and plotted against time as means  $\pm$  SE, as previously described (18, 35).

**Immunofluorescence staining.** EC grown on glass coverslips were fixed after the agonist treatment in 3.7% formaldehyde solution in PBS for 10 min at  $+4^{\circ}\text{C}$ , washed three times with PBS, permeabilized with PBS containing 0.2% Tween 20 (PBS-T) and 0.2% Triton X-100 for 30 min at room temperature, and blocked with 2% BSA in PBS-T for 30 min. Incubation with  $\beta$ -catenin antibodies was performed in 2% BSA in PBS-T for 1 h at room temperature followed by staining with Alexa 488-conjugated secondary antibodies. Actin filaments were stained with Texas red-conjugated phalloidin for 1 h at room temperature. After immunostaining, the glass slides were analyzed using a Nikon video imaging system (Nikon Instech) consisting of an inverted Nikon Eclipse TE300 microscope with an epifluorescence module, using a  $\times 60/1.40$  oil objective connected to a SPOT RT monochrome digital camera and image processor (Diagnostic Instruments, Sterling Heights, MI). The images were recorded and processed using Adobe Photoshop 7.0 software (Adobe Systems, San Jose, CA).

**Rho and Rac activation assays.** Activation of Rho and Rac GTPases in pulmonary EC culture was analyzed using Rho and Rac in vitro pull-down assay kits available from Upstate Biotechnology (Lake Placid, NY) according to the manufacturer's protocols, as previously described (2, 40).

**Immunoblotting.** After stimulation, cells were lysed and protein extracts were separated by SDS-PAGE, transferred to nitrocellulose membrane, and probed with specific antibodies as previously described (3, 7, 9). Intensities of immunoreactive protein bands were quantified using ImageQuant software (Molecular Dynamics, Sunnyvale, CA).

Fig. 2. Effect of OxPAPC, OxPAPS, and OxPAPA on EC actin cytoskeleton. EC monolayers grown on glass coverslips and treated with OxPAPC, OxPAPS, or OxPAPA ( $20\ \mu\text{g}/\text{ml}$ , 30 min) were fixed and subjected to immunofluorescence staining for F-actin with Texas red-phalloidin, as described in MATERIALS AND METHODS. Accumulation of F-actin at the cell periphery is marked by arrows. Results are representative of 3 independent experiments.



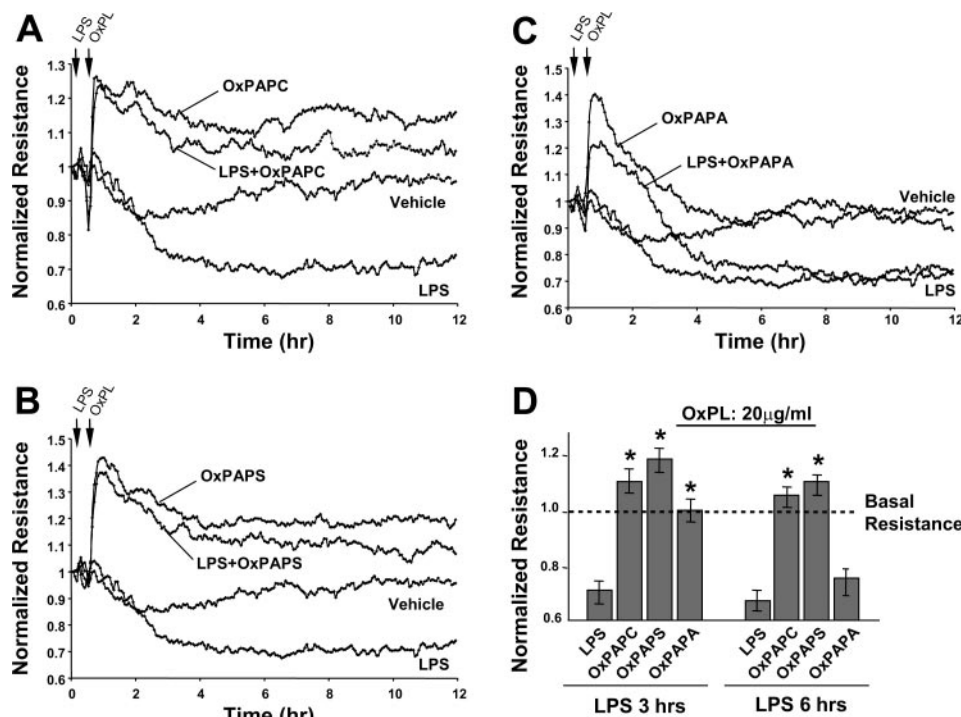


Fig. 3. Effect of OxPLs on LPS-induced endothelial barrier dysfunction. A–C: pulmonary EC were grown on gold microelectrodes. At the time point indicated by the first arrow, cells were pretreated with LPS (200 ng/ml, 20 min), followed by stimulation with 20 µg/ml OxPAPC (A), OxPAPS (B), or OxPAPA (C), as indicated by the second arrow, and TER was monitored for 12 h. D: summary of time-dependent effects of OxPLs on LPS-induced EC permeability. TER was measured at 3 or 6 h of LPS challenge. Results are representative of 3–5 independent experiments. Data are represented as means (SD).

*In vivo model of ALL.* Adult male C57BL/6J mice, 8–10 wk old, with an average weight of 20–25 g (Jackson Laboratories), were anesthetized with intraperitoneal injection of ketamine (75 mg/kg) and acepromazine (1.5 mg/kg). LPS (0.7 mg/kg body wt; *Escherichia coli* O55:B5) or sterile water was injected intratracheally in a small volume (20–30 µl) using a 20-gauge catheter (Penn-Century, Philadelphia, PA). Mice were randomized to concurrently receive sterile saline solution and OxPAPC (1.5 mg/kg) or OxPAPS (1.5 mg/kg) by intravenous injection in the external jugular vein to yield the following experimental groups: control, LPS only, OxPAPC (1.5 mg/kg) only, OxPAPS (1.5 mg/kg) only, LPS + OxPAPC (1.5 mg/kg), and LPS + OxPAPS (1.5 mg/kg). At 16 h, animals were killed by exsanguination under anesthesia. Tracheotomy was performed, and the trachea was cannulated with a 20-gauge intravenous catheter that was tied into place. Bronchoalveolar lavage fluid (BAL) was performed using 1 ml of sterile Hanks’ balanced salt buffer. The collected lavage fluid was centrifuged at 2,500 rpm for 20 min at +4°C, and the supernatant was removed and frozen at –80°C for subsequent protein study. The cell pellet was then resuspended in 1 ml of red blood cell lysis buffer (ACK Lysing Buffer; BioSource International) for 5 min and then repelleted by centrifugation at 2,500 rpm for 20 min at +4°C. The cell pellet was then resuspended in 200 µl of PBS, from which 20 µl of cell suspension were used for cell counting with a standard hemocytometer technique. The remaining 180 µl of cell suspension were repelleted by centrifugation, and cell pellets were stored at –80°C for subsequent detection of myeloperoxidase activity (MPO), as described elsewhere (38). Briefly, cell pellets were subjected to a round of freezing (on dry ice) and thawing (at room temperature), followed by 20-s sonication (Virsonic V60) at full power on ice. Samples were centrifuged at 10,000 g for 10 min at +4°C, and the supernatant was collected into fresh 1.5-ml tubes placed on ice. Next, 100 µl of supernatant were added to a polystyrene cuvette, and the MPO reaction was initiated by adding 2.9 ml of 1× assay buffer (50 mM potassium phosphate buffer, pH 6.0, containing 0.167 mg/ml *o*-dianisidine and 0.0005% H<sub>2</sub>O<sub>2</sub>). Changes in absorbance at 460 nm were recorded for 1 min with a spectrophotometer (Shimadzu UV 1201), and the rate of change (in absorbance/min) was converted to MPO activity. The BAL protein concentration was

determined using a modified Lowrey colorimetric assay with a Bio-Rad DC protein assay kit (Bio-Rad Laboratories, Hercules, CA). The absorbance was measured at 750 nm, and protein concentration was determined using standard curves.

*Statistical analysis.* Results are expressed as means ± SE of 3–10 independent experiments. Stimulated samples were compared with controls by using unpaired Student’s *t*-test. For multiple-group comparisons, a one-way ANOVA, followed by the post hoc Fisher’s test, was used. *P* < 0.05 was considered statistically significant.

**RESULTS**

*Polar head groups of OxPLs determine protective effects on endothelial permeability and cytoskeletal remodeling.* HPAEC monolayers were treated with 10, 20, or 50 µg/ml OxPAPC, OxPAPS, and OxPAPA followed by measurements of TER for 4 h in parallel experiments. EC stimulation with 10 or 20 µg/ml OxPAPC induced a sustained increase in TER (Fig. 1A). Consistent with previous findings (2), a further increase in OxPAPC concentration (50 µg/ml) caused an acute TER decrease followed by partial restoration. In contrast to OxPAPC, OxPAPS at 50 µg/ml did not cause a barrier-disruptive effect but, instead, promoted further TER elevation compared with 20 µg/ml (Fig. 1B). The barrier-disruptive effect observed in EC treated with 50 µg/ml OxPAPC was not detected in cells treated with even higher OxPAPS doses (up to 100 µg/ml OxPAPS; data not shown). Stimulation of HPAEC with OxPAPA induced a rapid dose-dependent increase in TER (Fig. 1C). Similarly to OxPAPS, high OxPAPA concentrations (50 µg/ml, Fig. 1C, and 100 µg/ml, data not shown) did not induce a barrier-disruptive effect. In contrast, OxPAPA induced a potent (50% increase) but transient elevation of TER with a peak at 30 min and a decline to nearly basal levels by 2.5 h posttreatment. Treatment of EC with nonoxidized PAPC, PAPS, and PAPA (Fig. 1, A–C, right) showed that none of the non-OxPLs exhibited barrier protective properties. These re-

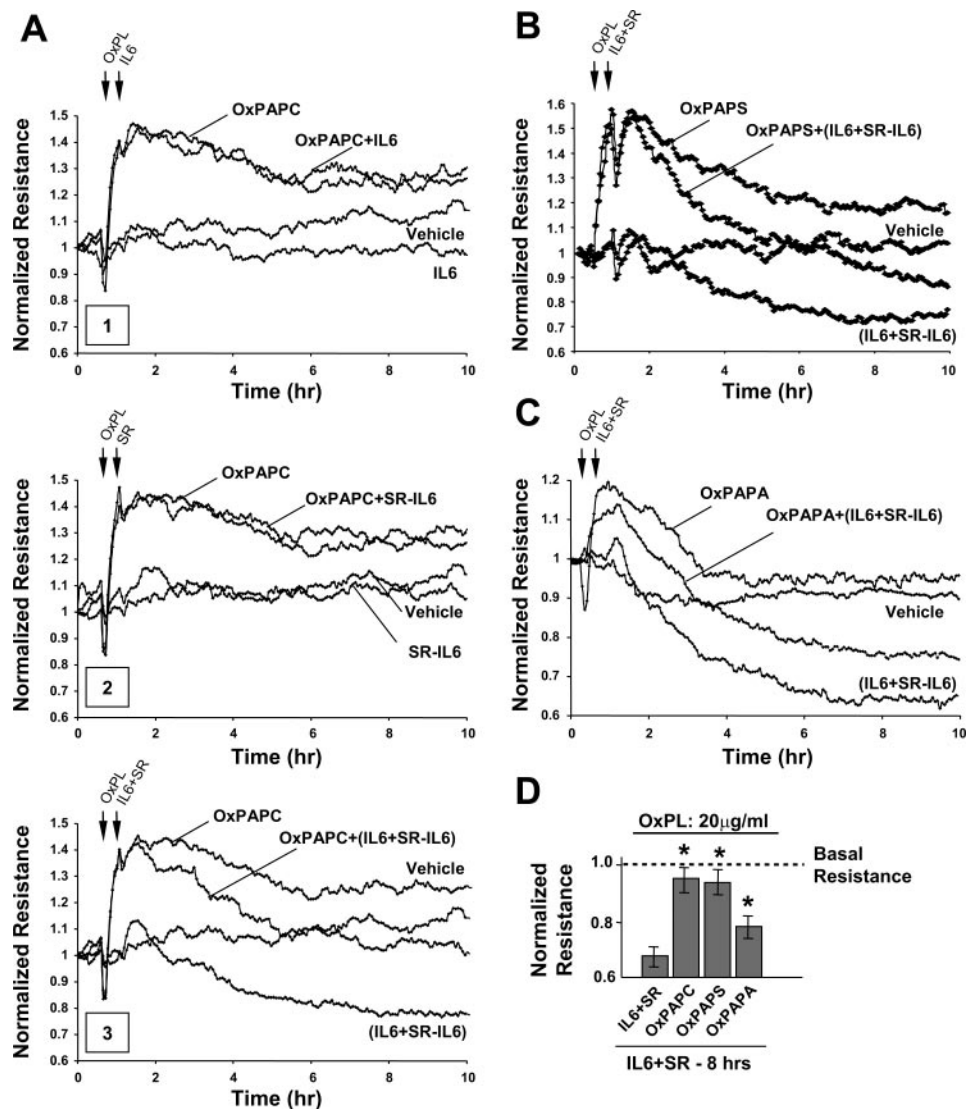
sults are consistent with previous studies (2) and suggest that oxidation is essential for barrier-protective effects of the phospholipids used in this study. Dose-dependent effects of OxPLs on EC barrier properties are summarized in Fig. 1D and show that only OxPAPS exhibited a pronounced and sustained barrier-protective effect at high concentrations (50  $\mu\text{g/ml}$ ). At lower concentrations, both OxPAPC and OxPAPS caused a sustained TER increase observed even after 2.5 h of stimulation, whereas OxPAPA induced a potent but transient barrier-protective response (Fig. 1E).

To further characterize effects of OxPLs on barrier regulation, we analyzed the remodeling of the actin cytoskeleton after EC stimulation with OxPAPC, OxPAPS, and OxPAPA (20  $\mu\text{g/ml}$ , 30 min). F-actin staining of stimulated EC was performed using Texas red-phalloidin as described in MATERIALS AND METHODS. OxPAPC and OxPAPS induced the most pronounced actin remodeling, characterized by the disappearance of stress fibers and the accumulation of F-actin at the cell periphery, whereas OxPAPA caused less dramatic cytoskeletal changes (Fig. 2). We have previously described the formation of unique ziplike actin projections that formed an intercollated

peripheral actin cytoskeletal structure in OxPAPC-treated cells (2). Similar peripheral actin structures have been observed in OxPAPS- but not OxPAPA-treated EC (Fig. 2). We speculate that the OxPAPA-caused lamellipodia formation shown in Fig. 2 can contribute to a rapid and transient increase in resistance, whereas the formation of ziplike actin projections mediates sustained enhancement of the EC barrier. Consistent with results of TER measurements, non-OxPLs had no effect on the EC cytoskeleton (data not shown).

*Effects of OxPLs with different polar head groups on endothelial barrier dysfunction induced by inflammatory mediators.* We and others have previously reported that OxPAPC exhibited a protective effect against LPS-induced lung inflammation and pulmonary EC barrier dysfunction. This effect was linked to concurrent inhibition of TLR4-dependent pathway by OxPAPC (10, 11). In this study, we tested effects of OxPLs on LPS-induced endothelial barrier dysfunction in the cultured human pulmonary endothelial monolayers. Cells were pretreated with LPS (200 ng/ml, 20 min) and then stimulated with OxPAPC, OxPAPS, or OxPAPA (20  $\mu\text{g/ml}$ ). OxPAPC and OxPAPS pretreatment blunted EC permeability increases in

Fig. 4. Effect of OxPLs on IL-6-induced barrier dysfunction. A–C: at the time point indicated by the second arrow, pulmonary EC pretreated with 20  $\mu\text{g/ml}$  OxPAPC (A), OxPAPS (B), or OxPAPA (C), as indicated by the first arrow, were stimulated with IL-6 (IL6; 20 ng/ml) alone (A1), IL-6 soluble receptor (SR-IL6; 100 ng/ml) alone (A2), or a combination of IL-6 (20 ng/ml) and SR-IL-6 (100 ng/ml) (IL+SR-IL6; A3, B, and C), as indicated by the second arrow, and measurements of TER were performed for 10 h across confluent EC monolayers. D: comparison of time-dependent effects of OxPLs on IL-6/IL-6-SR-induced EC permeability. TER was measured after 8 h of agonist stimulation. Results are representative of 3–5 independent experiments. Data are represented as means (SD).



response to LPS (Fig. 3, A and B), whereas OxPAPA only partially attenuated LPS-induced EC barrier dysfunction, and its protective effect disappeared after 5 h of LPS stimulation (Fig. 3C). Complete inhibition of the LPS-induced permeability response was not achieved even at higher OxPAPA concentrations (up to 100  $\mu\text{g/ml}$ ; data not shown). A summary of TER measurements (Fig. 3D) illustrates that only OxPAPC and OxPAPS exhibited sustained and complete protective effects against LPS-induced EC dysfunction. It is important to note that treatment of LPS-challenged EC monolayers with OxPAPC and OxPAPS not only blunted LPS-induced TER decline but also caused sustained TER elevation above the baseline. Non-OxPLs had no effect on basal TER levels and LPS-induced TER changes (data not shown). These results and published data (2, 10, 31, 35) clearly indicate that protective effects of OxPAPC and OxPAPS involve two mechanisms: inhibition of an LPS-induced, TLR4-mediated cascade of EC barrier dysfunction and direct and rapid enhancement of EC barrier properties via Rac/Cdc42-mediated EC cytoskeletal remodeling, which is addressed in more detail in the DISCUSSION.

In the following studies, we examined potential protective effects of OxPLs in a model of barrier dysfunction induced by a well-recognized marker of inflammation, IL-6 (26, 35). Treatment of HPAEC with either IL-6 (25 ng/ml) or its soluble receptor (IL-6SR; 100 ng/ml) alone did not significantly change basal resistance or affect the OxPAPC-mediated TER increase (Fig. 4A). In contrast, the combination of IL-6 and IL-6-SR induced a significant TER decrease. Pretreatment of EC monolayers with OxPAPC partially attenuated IL-6/IL-6-SR-induced permeability; however, it still restored TER to the values registered in nonstimulated EC. OxPAPS pretreatment exerted similar effects on the IL-6/IL-6-SR-induced permeability increase (Fig. 4B). OxPAPA was less potent in reduction of IL-6/IL-6-SR-induced permeability (Fig. 4C). Non-OxPLs had no effect on basal TER levels and IL-6/IL-6-SR-induced TER changes (data not shown). A comparison of protective effects by different OxPLs is summarized in Fig. 4D. These results strongly suggest more potent protective effects of OxPAPC and OxPAPS, compared with OxPAPA, against the endothelial barrier dysfunction induced by inflammatory agents in vitro. In the next experiments, we evaluated protective effects of OxPAPC and OxPAPS in the murine model of LPS-induced lung injury.

**Effects of OxPAPC and OxPAPS on LPS-induced lung barrier dysfunction.** Intratracheal LPS induced a prominent acute inflammatory response in the lung (Fig. 5A) with a dramatic increase in BAL total cell counts at 18 h ( $3.07 \pm 0.24 \times 10^6$  compared with  $1.17 \pm 0.52 \times 10^5$  cells/ml in LPS-untreated controls,  $P < 0.001$ ). The LPS-induced increase in BAL cell count was significantly attenuated by OxPAPC and OxPAPS ( $1.88 \pm 0.23 \times 10^6$  and  $1.09 \pm 0.07 \times 10^6$  cells/ml, respectively, vs.  $3.07 \pm 0.24 \times 10^6$  cells/ml for LPS alone,  $P < 0.05$ ), whereas treatment with nonoxidized PAPC did not significantly reduce BAL cell counts (data not shown), similar to the results we have previously described (35). Consistent with effects on BAL total cell counts, OxPAPC and OxPAPS treatment dramatically decreased the levels of MPO activity (Fig. 5B), which reflect neutrophil activation in the BAL samples. Importantly, OxPAPS was significantly more potent

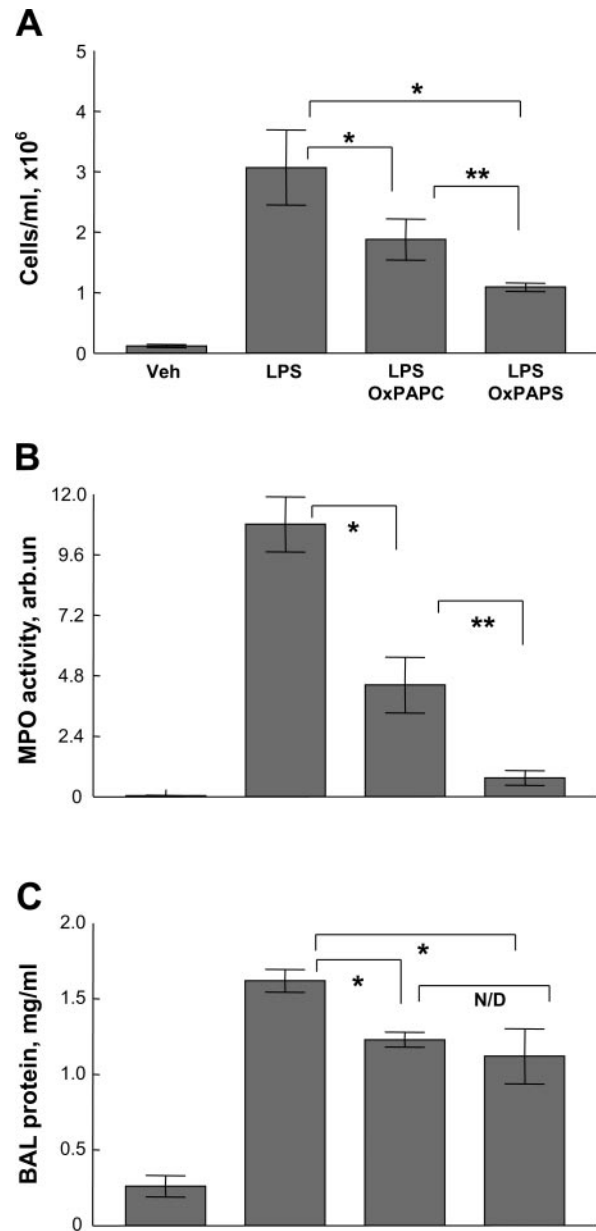


Fig. 5. Intravenous OxPAPC and OxPAPS attenuate LPS-induced neutrophil accumulation in bronchoalveolar lavage (BAL) fluid, increased myeloperoxidase (MPO) activity, and lung barrier dysfunction. Intratracheal LPS (0.7 mg/kg) or sterile water (vehicle, Veh) was administered 18 h before cytological analysis of BAL fluid and measurements of MPO activity. LPS induced a dramatic increase in BAL total cell count (A) and MPO activity in BAL cell pellets (B) that was markedly attenuated by intravenous OxPAPC and OxPAPS (1.5 mg/kg). There were no significant differences in cell counts and MPO activity between animals treated with vehicle or OxPAPC alone (data not shown). BAL protein concentration was assessed at 18 h after intratracheal LPS challenge or sham injection. Intravenous OxPAPC and OxPAPS (1.5 mg/kg) significantly reduced the pronounced increase in BAL protein caused by LPS administration. Data are represented as means  $\pm$  SE;  $n = 6-9$  per group. \* $P < 0.01$ ; \*\* $P < 0.05$ . N/D, no significant difference; arb. un., arbitrary units.

than OxPAPC in attenuating the LPS-induced increases in cell counts and MPO activity (Fig. 4, A and B).

Next, using BAL protein content as a marker of barrier disruption and lung injury, we examined the effects of OxPAPC and OxPAPS on LPS-induced lung edema. Intratra-

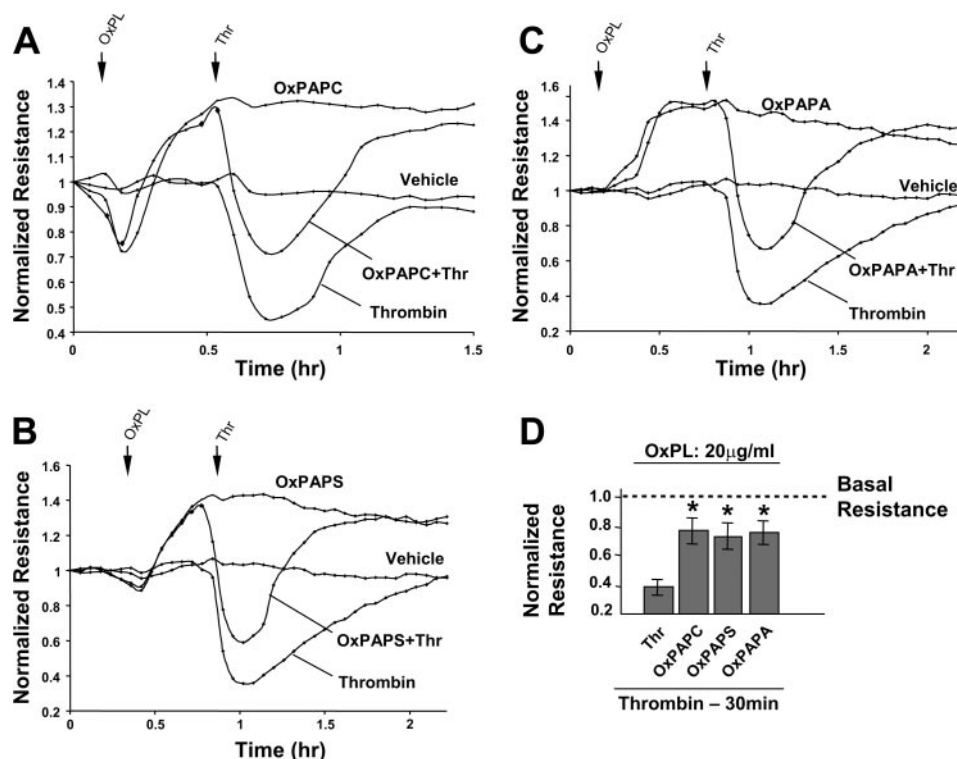
cheal challenge with LPS significantly increased the total protein concentration in BAL fluid compared with that in control animals ( $1.62 \pm 0.08$  vs.  $0.26 \pm 0.15$  mg/ml,  $P < 0.005$ ) (Fig. 5C). Concurrent treatment with intratracheal LPS and intravenous OxPAPC or OxPAPS significantly attenuated BAL protein concentrations compared with LPS alone ( $1.23 \pm 0.05$  and  $1.12 \pm 0.18$  mg/ml, respectively, vs.  $1.62 \pm 0.08$  mg/ml,  $P < 0.001$ ). There was no significant difference in BAL protein between OxPAPC-treated animals and controls in the absence of LPS. These results strongly suggest the protective effects of OxPAPC and OxPAPS against LPS-induced lung vascular barrier dysfunction *in vivo*.

Our data suggest that although both OxPAPC and OxPAPS induced sustained barrier protective effects *in vivo* and *in vitro*, OxPAPS was more potent in the attenuation of LPS-induced lung inflammation *in vivo*. Importantly, in contrast to OxPAPC, which at doses above  $30 \mu\text{g/ml}$  lost barrier-protective properties (Fig. 1A and Ref. 2), OxPAPS exhibited a prominent protective effect at  $50 \mu\text{g/ml}$  (Fig. 1B) and up to  $100 \mu\text{g/ml}$  (data not shown). Because OxPAPS displayed a wider barrier-protective concentration range *in vitro* and *in vivo*, in the following experiments we used OxPAPS to study the molecular mechanisms underlying its barrier-protective effects in pulmonary EC.

*Characterization of barrier protective properties of OxPLs bearing different polar head groups in a thrombin model of pulmonary EC hyperpermeability.* HPAEC monolayers were pretreated with OxPAPC, OxPAPS, or OxPAPA ( $20 \mu\text{g/ml}$ , 30 min), followed by thrombin challenge ( $0.5 \text{ U/ml}$ ). OxPAPC, OxPAPS, and OxPAPA exhibited similar protective effects in the acute EC permeability response to thrombin (Fig. 6). Moreover, these three OxPLs not only significantly attenuated permeability increase in the response to thrombin but also,

during the recovery phase, elevated resistance to much higher levels above the baseline. Next, we used OxPAPS, which exhibited protective effects in all three models of the pulmonary EC barrier dysfunction, as an example to characterize effects of barrier-protective OxPLs on cytoskeletal remodeling. Confluent HPAEC monolayers were pretreated with OxPAPS ( $20 \mu\text{g/ml}$ , 30 min), followed by thrombin stimulation ( $0.5 \text{ U/ml}$ ). Remodeling of actin cytoskeleton and adherens junctions was analyzed at the peak of barrier dysfunction (30 min) and during the recovery phase (50 min) after thrombin challenge. Cells were stained with Texas red-phalloidin to visualize F-actin and with antibody against adherens junction protein  $\beta$ -catenin. EC stained at the peak of thrombin-induced barrier dysfunction showed dramatic paracellular gap formation (indicated by arrows), stress fiber formation, and cell contraction compared with nonstimulated EC monolayers (Fig. 7A). OxPAPS pretreatment induced enhancement of peripheral actin and significantly suppressed thrombin-induced paracellular gap formation at 30 min. During the recovery phase, OxPAPS promoted disappearance of stress fibers accompanied by accumulation of actin at the areas of cell periphery, whereas EC monolayers treated with thrombin alone (50 min) exhibited a significant number of stress fibers and paracellular gaps (Fig. 7A). Consistent with these results, OxPAPS pretreatment also preserved a continuous adherens junction pattern, visualized by  $\beta$ -catenin staining, after 30 min of thrombin stimulation and did cause a complete recovery of adherens junction pattern by 50 min after thrombin stimulation (Fig. 7B). Similar results were obtained when OxPAPC was used instead of OxPAPS (data not shown). In contrast, EC monolayers stimulated with thrombin alone displayed massive disruption of cell-cell contacts after 30 min and only partial recovery after 50 min of thrombin treatment (Fig. 7B).

Fig. 6. Effect of OxPL preincubation on thrombin-induced barrier dysfunction. Pulmonary EC were preincubated with  $20 \mu\text{g/ml}$  OxPAPC (A), OxPAPS (B), or OxPAPA (C) for 30 min, followed by thrombin ( $0.5 \text{ U/ml}$ ) challenge, and TER changes were monitored over the time. D: summary of OxPL effects on thrombin-induced EC permeability. Results are representative of 5–10 independent experiments. Data are represented as means (SD). Thr, thrombin.



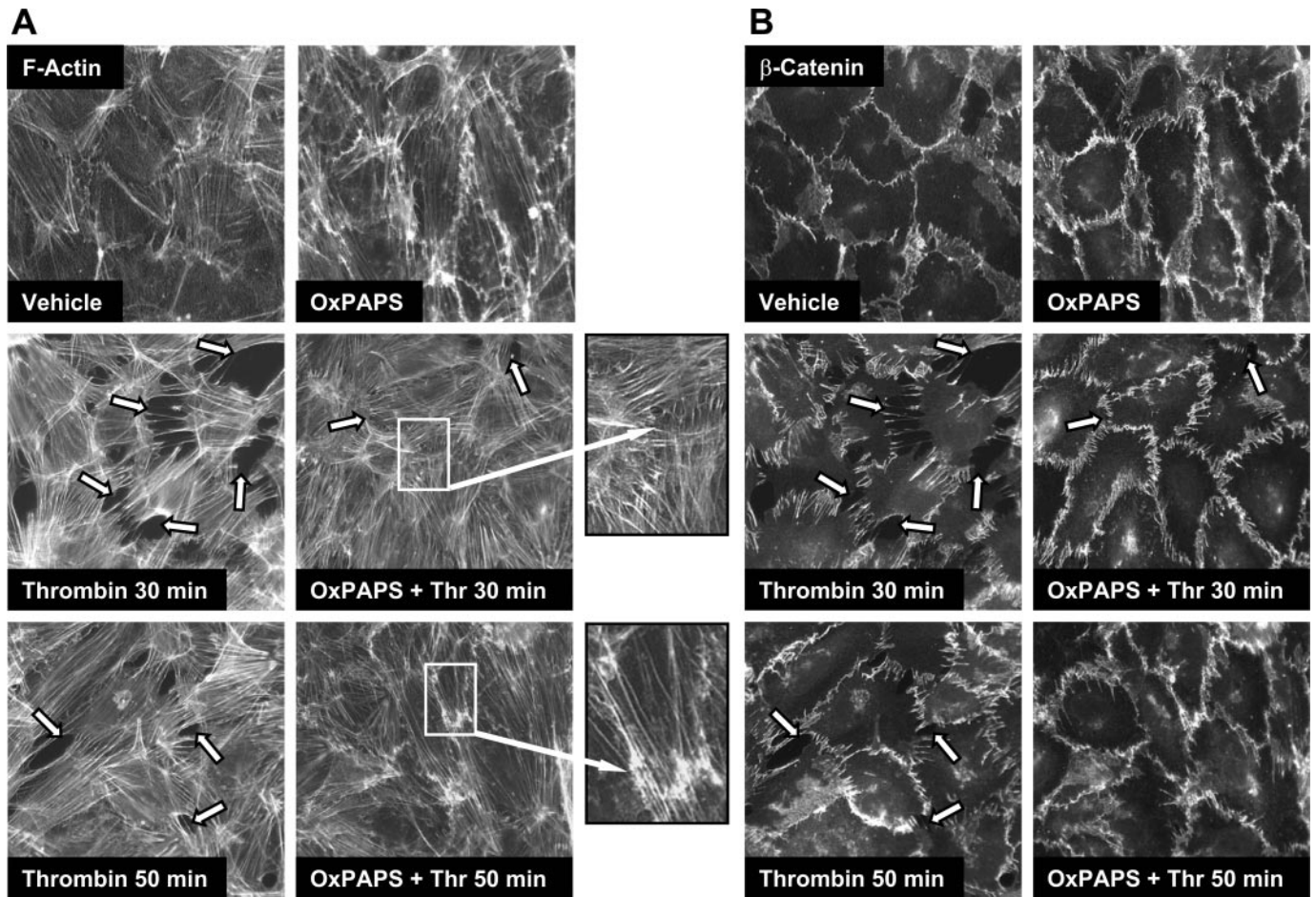


Fig. 7. Effect of OxPAPS on thrombin-induced cytoskeletal remodeling and adherens junction integrity. EC grown on glass coverslips were incubated with OxPAPS (20  $\mu\text{g/ml}$ , 30 min), followed by thrombin (0.5 U/ml) treatment for 30 or 50 min. Cells were fixed, and double immunofluorescence staining was performed according to the protocol described in MATERIALS AND METHODS. Cells were probed with Texas red-phalloidin to detect actin filaments (A) and with  $\beta$ -catenin antibody to label adherens junctions (B). Paracellular gaps are marked by arrows. Insets depict higher magnification images of cell-cell contacts. Results are representative of 3 independent experiments.

In complementary series of experiments, HPAEC were treated with combination of thrombin (0.5 U/ml) and OxPAPS (20  $\mu\text{g/ml}$ ) for 5 or 50 min and used for immunofluorescence analysis of cytoskeletal remodeling. In this setting, OxPAPS (Fig. 8A) did not prevent the acute phase of EC barrier dysfunction (5 min of combined thrombin and OxPAPC treatment) but significantly promoted barrier restoration during the recovery phase at 50 min of treatment, which was characterized by a reduction in the number of paracellular gaps (indicated by arrows) and enhanced F-actin accumulation in the cell cortical area (Fig. 8A, insets). These morphological changes were consistent with the TER measurements made under the same experimental conditions (Fig. 8B), which showed enhanced TER recovery in cells cotreated with thrombin and OxPAPS compared with that in cells treated with thrombin alone. Non-OxPLs had no effect on thrombin-induced TER changes and cytoskeletal remodeling (data not shown).

*Effect of OxPAPS on thrombin-induced Rho activation and myosin light chain phosphorylation.* We and others have previously described the essential role of the small GTPases Rho and Rac in the regulation of endothelial barrier (2, 9, 13, 19, 42, 43), and Rho-dependent pathway was described as a major mechanism of thrombin-induced endothelial barrier dysfunction

(9, 13, 19, 43). In this study, EC were pretreated with OxPAPS (20  $\mu\text{g/ml}$ , 30 min) followed by thrombin challenge (0.5 U/ml, 15 min or 30 min), and changes in Rho and Rac activation were monitored over the time (Fig. 9A). Rho activity induced by thrombin was significantly elevated at 15 and 30 min. Rac activity was decreased below the basal levels after 15 min and was only slightly elevated after 30 min of thrombin treatment. Remarkably, OxPAPS pretreatment significantly attenuated Rho activation after 15 min of thrombin stimulation and completely abolished Rho activation after 30 min compared with thrombin alone. In addition, OxPAPC prevented initial thrombin-induced Rac inactivation and dramatically enhanced Rac activation by 30 min of thrombin stimulation. Treatment with OxPAPS alone induced robust Rac activation without noticeable activation of Rho. Similar results were obtained when OxPAPC was used instead of OxPAPS (data not shown).

Because phosphorylation of regulatory myosin light chains (MLC) is mediated by a Rho pathway via Rho kinase-induced phosphorylation and inactivation of MLC phosphatase (19), we then investigated effects of OxPAPS on thrombin-induced MLC phosphorylation. Thrombin (0.5 U/ml, 15 min) induced a pronounced increase in MLC phosphorylation, whereas

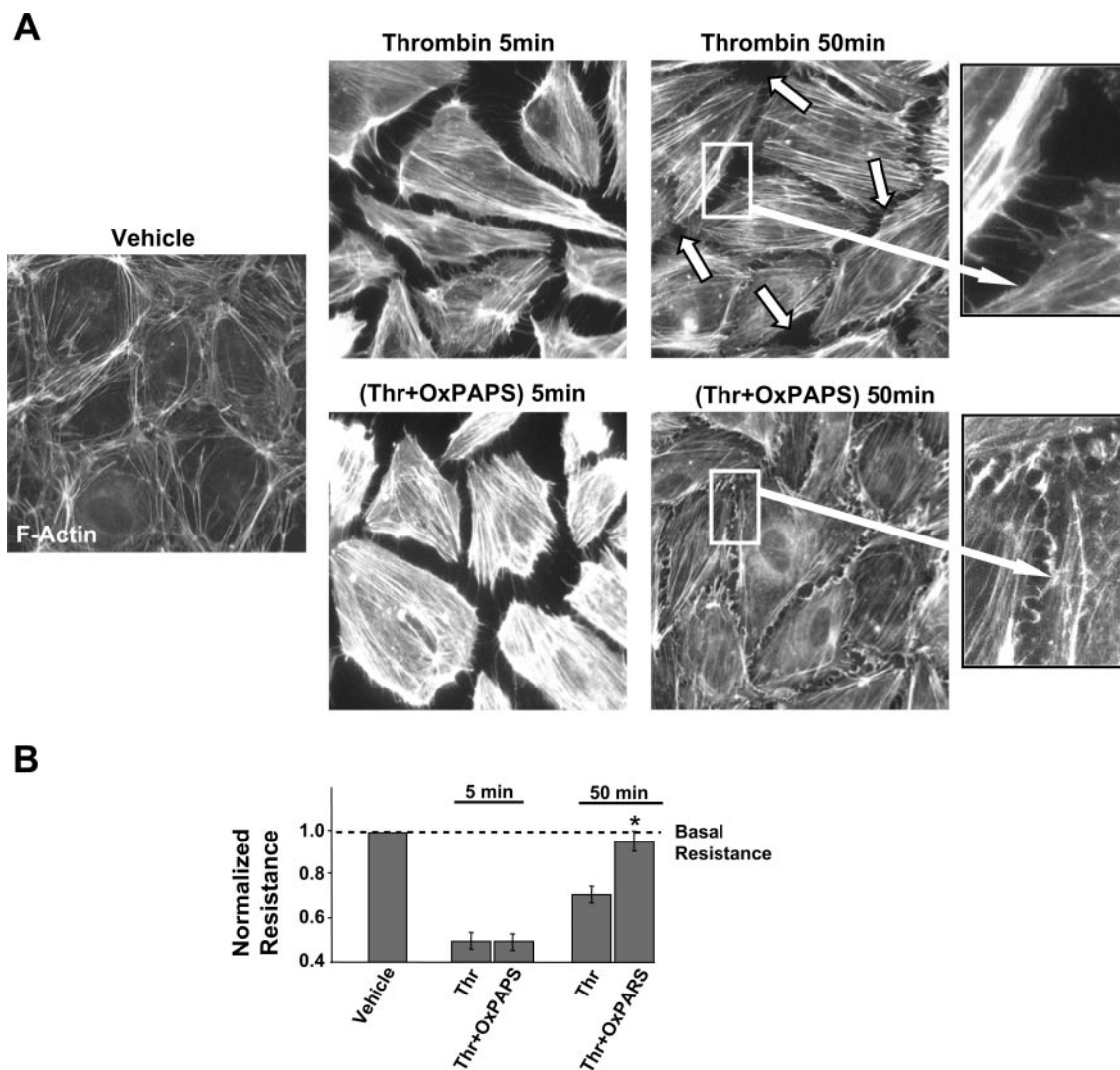


Fig. 8. Effect of combined stimulation with thrombin and OxPAPS on EC monolayer integrity and TER. A: EC grown on glass coverslips and treated with combination of thrombin (0.5 U/ml) and OxPAPS (20  $\mu$ g/ml) for 15 or 50 min were fixed and subjected to immunofluorescent staining for F-actin with Texas red-phalloidin. Insets represent higher magnification images of the areas of cell-cell contacts. Results are representative of 3 independent experiments. B: TER was monitored across the confluent EC monolayers treated with a combination of thrombin (0.5 U/ml) and OxPAPS (20  $\mu$ g/ml). Data represent results of TER measurements after 5 and 50 min of stimulation.

OxPAPS (20  $\mu$ g/ml, 30 and 15 min; data not shown) was without effect (Fig. 9B). Remarkably, EC pretreatment with OxPAPS significantly reduced MLC phosphorylation in response to thrombin. Similar results were obtained when OxPAPC was used instead of OxPAPS, whereas non-OxPLs had no effect on thrombin-induced Rho activation and MLC phosphorylation (data not shown). These experiments strongly suggest that OxPLs tested in this study exhibit the protective effect against edemagenic agonists via modulation of Rho-dependent pathway of EC barrier dysfunction.

#### DISCUSSION

The results of this study demonstrate for the first time the important role of polar head groups in the protective effects elicited by oxidized phospholipids in the *in vitro* and *in vivo* models of EC barrier dysfunction. The concentrations of OxPLs *in vivo* under physiological conditions and during inflammation are unclear. Because of the structural diversity of

OxPLs and the presence of a high excess of non-OxPLs, quantitation of OxPLs *in vivo* represents a major challenge for analytical techniques. Therefore, the estimates of *in vivo* concentrations are sparse, and most publications compare healthy and diseased tissues without providing absolute concentrations of analyzed OxPLs. OxPLs were studied mainly in the context of chronic inflammation characteristic of atherosclerosis. Published studies provide an estimate of 400  $\mu$ g of combined active PCs (containing both fragmented and full-length oxidized residues) per gram of atherosclerotic vascular tissue (49). The concentration of isoprostane-containing OxPLs, which demonstrated the most prominent barrier-protective effects in our experiments (2), was estimated in human atherosclerotic lesions in the range of 30–100 ng/g wet wt and was significantly higher than in healthy human vessels (1 ng/g wet wt) (20, 44, 49). There are no published quantitative estimates of OxPLs levels in lung. In humans, semiquantitative immunohistochemical methods demonstrated accumulation of OxPL in

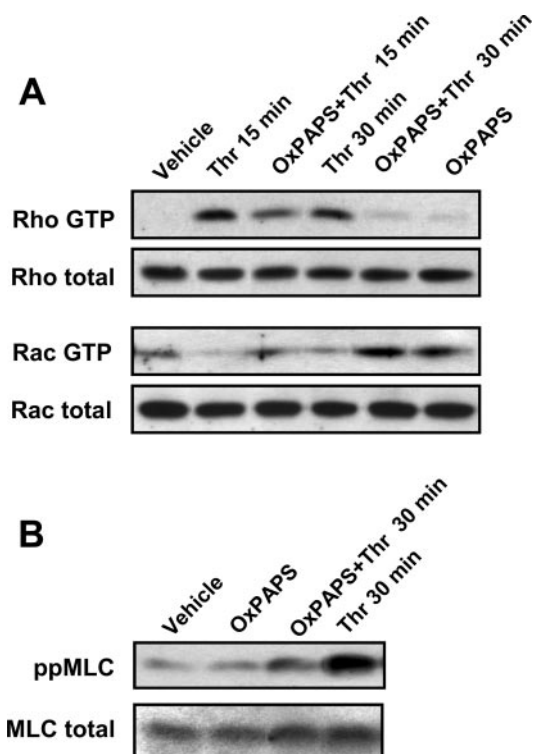


Fig. 9. Effect of OxPAPS and thrombin on Rho and Rac activities and myosin light chain (MLC) phosphorylation. Pulmonary EC were pretreated with OxPAPS (20  $\mu$ g/ml, 30 min), followed by thrombin challenge (0.5 U/ml, 15 or 30 min). A: Rho and Rac activities were measured using pull-down activation assays, as described in MATERIALS AND METHODS. B: phosphorylation of MLC (ppMLC) was detected by Western blot analysis with specific antibody. Equal protein loading was confirmed by reprobing of membranes with MLC antibody. Results are representative of 3 independent experiments.

lung during inflammation. The presence of several OxPL species in mouse lung tissue has been demonstrated using mass spectrometry and was significantly increased by tissue oxidative stress (34). Generation of OxPLs in lung is likely to be a by-product of oxidative burst produced by activated leukocytes. Indeed, activated neutrophils and monocytes stimulated oxidation of PAPC with predominant accumulation of epoxyisoprostane-PC, which achieved a concentration of 200 nM (25). This study shows that OxPLs at concentrations equivalent to micromolar concentrations of isoprostane-PL induce a prominent barrier-protective effect in pulmonary EC. Other reports indicate that epoxyisoprostane-containing PC elevates cAMP levels known to increase endothelial barrier function at concentrations as low as 100 ng/ml (29). In conclusion, several experimental groups have documented the presence of OxPLs in vivo, as well as elevation of local and systemic levels of OxPL during various types of acute and chronic inflammation. Direct measurements of absolute OxPL levels in lung have not been performed yet. However, experimental data obtained for different models of acute and chronic tissue inflammation suggest that OxPLs are likely to reach concentrations sufficient to support pulmonary endothelial function in vivo.

OxPAPC and OxPAPS containing positively and negatively charged polar head groups, respectively, showed sustained barrier-protective effects on pulmonary EC, whereas OxPAPA lacking a head group caused a potent but transient TER increase. A recent report by Li et al. (29) indicated that

epoxyisoprostane-containing products of PAPC oxidation may engage prostaglandin E<sub>2</sub> (EP2) receptor and elevate intracellular cAMP levels, which in turn promote the endothelial barrier function, prevent agonist-induced permeability increases (8, 30, 33, 37, 39), and may contribute to the early phase of barrier enhancement in response to OxPLs. Elevation of cAMP and activation of cAMP-dependent protein kinase by OxPLs has been previously shown by us and other groups (3, 15, 28). Thus epoxyisoprostane groups contained in the products of PAPS, PAPC, and PAPA oxidation may induce transient EC barrier-protective responses via EP2-mediated elevation of intracellular cAMP. However, sustained protective effects of OxPAPC and OxPAPS not observed in OxPAPA-stimulated cells suggest an additional mechanism of barrier protective action, which requires the presence of polar head groups in the OxPL products. The precise mechanism of sustained protective effects by OxPLs containing polar head groups is not clear, and we speculate that it may involve a yet to be identified putative receptor(s) distinct from the prostaglandin receptor family. This receptor(s), unlike EP2, requires the presence of both an oxygenated arachidonoyl moiety and a polar head group for triggering a sustained barrier-protective response. In support of this notion, EC preincubation with the EP2 antagonist AH6809, which inhibited OxPAPC-induced activation of EP2 (29), had no effect on the OxPAPC- and OxPAPS-induced sustained barrier-protective response (data not shown).

The inhibitory effect of OxPAPC on LPS-induced inflammatory cascades is due to the ability of OxPAPC to suppress activation of the major LPS receptor TLR4 by inactivating the coreceptors LBP and CD14, which are essential for LPS interaction with TLR4 (1, 10). In the previous studies, we described a dose-dependent attenuation by OxPAPC of LPS-induced lung inflammation and vascular leak in the rat model of LPS-induced acute lung injury. The results of the present study show that both OxPAPC and OxPAPS dramatically attenuated leukocyte accumulation and MPO activation in the BAL upon intratracheal LPS instillation in vivo and abolished LPS-induced EC barrier dysfunction in vitro. Furthermore, cell culture experiments showed only partial attenuation of LPS-induced TER decline by OxPAPA, which lacks the head group. On the basis of our results, we speculate that complete inhibition of LPS-induced EC barrier dysfunction by OxPAPC and OxPAPS and only partial attenuation of LPS effects by OxPAPA may suggest an essential role for head polar groups in the competitive interaction with LBP. In addition to suppression of LPS-TLR4 signaling, OxPAPC also inhibits interactions of other proinflammatory stimuli such as bacterial ligands and CpG-rich DNA with TLR2 and TLR9 receptors, respectively (31, 45). Thus, similarly to OxPAPC, other OxPLs bearing polar head groups, including OxPAPS, also may inhibit inflammatory reactions mediated by other TLR family receptors, and further studies are required to explore these potential important effects.

OxPLs also partially attenuated IL-6-induced EC barrier dysfunction. The IL-6 receptor system is distinct from the TLR family and consists of two polypeptide chains, an 80-kDa IL-6 receptor (IL-6R) and a 130-kDa signal transducer (gp130). Similarly to activation of TLR4, which requires soluble receptor cofactors, the soluble IL-6R can form a stimulatory complex with IL-6, which associates with gp130 coreceptor and

triggers JAK-STAT, PI3-kinase/AKT, and MAP kinase signaling pathways (22). Although precise mechanisms of IL-6-mediated EC barrier dysfunction remain to be elucidated, IL-6-induced activation of MAP kinase pathways may represent a barrier-disruptive signaling cascade. Our results show that none of the OxPLs tested in this work blocked IL-6-induced barrier dysfunction; however, OxPLs increased TER in both vehicle- and IL-6-treated EC cultures in an additive fashion. Partial attenuation of IL-6-induced EC permeability decreases may be due to OxPL-induced activation of Rac/Cdc42 and peripheral actin cytoskeletal enhancement, described in our previous studies (2), which appear to be independent on proinflammatory signaling or MAP kinase activation induced by IL-6.

Our results demonstrate the ability of OxPLs to attenuate thrombin-induced MLC phosphorylation and hyperpermeability. Furthermore, barrier-protective effects of OxPAPC in the model of thrombin-induced EC barrier dysfunction are associated with the reduction of thrombin-induced Rho activation and stimulation of Rac signaling critical for EC barrier recovery (2, 7, 32). Upstream mechanisms of Rho regulation and Rho-Rac cross talk have been the focus of studies by several groups (7, 17, 41). The results of this study show attenuation of agonist-induced activation of the Rho pathway by OxPLs. OxPAPC stimulates protein kinase A (3, 28), which may suppress Rho activation via phosphorylation of Rho GDP dissociation inhibitor (RhoGDI) (39). Other mechanisms may involve modulation of Rho-specific guanosine nucleotide exchange factors (GEFs) by signal protein kinases (PKA, PKC, Src) activated by OxPAPC (3, 50). A recent report by Herband and Ahmadian (21) shows that Rac1 may inactivate Rho via a p190-RhoGAP (Rho-specific GTPase activating protein) mechanism. Studies by our group are underway to define upstream mechanisms of Rac/Cdc42 regulation by OxPLs and delineate a cross talk between Rac and Rho in OxPL-mediated signaling.

Assembly of adherens junctions is precisely regulated via Rac-dependent association of transmembrane protein VE-cadherin with the intracellular catenin complex, which links VE-cadherin with the cytoskeleton and provides physical integrity of the adherens junction complex (16). VE-cadherin- $\beta$ -catenin interaction is negatively regulated by actin- and  $\beta$ -catenin-binding protein IQGAP1. Activated Rac binds its effector IQGAP1 and promotes VE-cadherin- $\beta$ -catenin interaction (36). Enhanced Rac activation observed in the OxPAPC-pretreated cells after 30 min of thrombin stimulation may promote adherens junctions assembly and enhance adherens junction integrity, as observed in this study (Fig. 7B). Thus Rac-dependent enhancement of cortical actin cytoskeleton and adherens junction assembly may represent two complementary Rac-mediated mechanisms involved in the EC barrier recovery after challenge with barrier-disruptive agonists.

Thus our results demonstrate two modalities for biologically active OxPLs in protecting the pulmonary vascular endothelial barrier under acute pathological conditions: 1) via direct blunting of TLR-4 mediated inflammatory cascade and vascular endothelial barrier dysfunction, and 2) via stimulation of intrinsic EC barrier-protective mechanisms dependent on the cross talk between Rac and Rho pathways. Our data also suggest OxPAPC and OxPAPS as promising molecules for drug design and therapeutic treatment of ALI and ARDS.

Further analysis of bioactive compounds derived from these OxPLs may lead to the discovery of potent barrier-protective compounds that may be used in preventive therapies for treatment of acute lung injury.

#### ACKNOWLEDGMENTS

We thank Nurgul Moldobaeva and Eddie Chiang for superb laboratory assistance.

#### GRANTS

This work was supported by National Heart, Lung, and Blood Institute Grants HL076259 and HL075349 (to K. G. Birukov), American Heart Association Scientist Development Grant (to A. A. Birukova), the EU Molstroke project LSHM-CT-2004-005206, and a grant from Fonds zur Förderung Wissenschaftlichen Forschung (S9407-B11 to V. N. Bochkov).

#### REFERENCES

1. **Birukov KG.** Oxidized lipids: the two faces of vascular inflammation. *Curr Atheroscler Rep* 8: 223–231, 2006.
2. **Birukov KG, Bochkov VN, Birukova AA, Kawkitinarong K, Rios A, Leitner A, Verin AD, Bokoch GM, Leitinger N, Garcia JG.** Epoxycholestenone-containing oxidized phospholipids restore endothelial barrier function via Cdc42 and Rac. *Circ Res* 95: 892–901, 2004.
3. **Birukov KG, Leitinger N, Bochkov VN, Garcia JG.** Signal transduction pathways activated in human pulmonary endothelial cells by OxPAPC, a bioactive component of oxidized lipoproteins. *Microvasc Res* 67: 18–28, 2004.
4. **Birukova AA, Adyshev D, Gorshkov B, Bokoch GM, Birukov KG, Verin AA.** GEF-H1 is involved in agonist-induced human pulmonary endothelial barrier dysfunction. *Am J Physiol Lung Cell Mol Physiol* 290: L540–L548, 2006.
5. **Birukova AA, Birukov KG, Adyshev D, Usatyuk P, Natarajan V, Garcia JG, Verin AD.** Involvement of microtubules and Rho pathway in TGF- $\beta$ 1-induced lung vascular barrier dysfunction. *J Cell Physiol* 204: 934–947, 2005.
6. **Birukova AA, Birukov KG, Smurova K, Adyshev DM, Kaibuchi K, Alieva I, Garcia JG, Verin AD.** Novel role of microtubules in thrombin-induced endothelial barrier dysfunction. *FASEB J* 18: 1879–1890, 2004.
7. **Birukova AA, Chatchavalvanich S, Rios A, Kawkitinarong K, Garcia JG, Birukov KG.** Differential regulation of pulmonary endothelial monolayer integrity by varying degrees of cyclic stretch. *Am J Pathol* 168: 1749–1761, 2006.
8. **Birukova AA, Liu F, Garcia JG, Verin AD.** Protein kinase A attenuates endothelial cell barrier dysfunction induced by microtubule disassembly. *Am J Physiol Lung Cell Mol Physiol* 287: L86–L93, 2004.
9. **Birukova AA, Smurova K, Birukov KG, Kaibuchi K, Garcia JGN, Verin AD.** Role of Rho GTPases in thrombin-induced lung vascular endothelial cells barrier dysfunction. *Microvasc Res* 67: 64–77, 2004.
10. **Bochkov VN, Kadl A, Huber J, Gruber F, Binder BR, Leitinger N.** Protective role of phospholipid oxidation products in endotoxin-induced tissue damage. *Nature* 419: 77–81, 2002.
11. **Bochkov VN, Leitinger N.** Anti-inflammatory properties of lipid oxidation products. *J Mol Med* 81: 613–626, 2003.
12. **Bochkov VN, Leitinger N, Birukov KG.** Role of oxidized phospholipids in acute lung injury. *Curr Respir Med Rev* 2: 27–37, 2006.
13. **Carbajal JM, Schaeffer RC Jr.** RhoA inactivation enhances endothelial barrier function. *Am J Physiol Cell Physiol* 277: C955–C964, 1999.
14. **Chabot F, Mitchell JA, Gutteridge JM, Evans TW.** Reactive oxygen species in acute lung injury. *Eur Respir J* 11: 745–757, 1998.
15. **Cole AL, Subbanagounder G, Mukhopadhyay S, Berliner JA, Vora DK.** Oxidized phospholipid-induced endothelial cell/monocyte interaction is mediated by a cAMP-dependent R-Ras/PI3-kinase pathway. *Arterioscler Thromb Vasc Biol* 23: 1384–1390, 2003.
16. **Dejana E.** Endothelial cell-cell junctions: happy together. *Nat Rev Mol Cell Biol* 5: 261–270, 2004.
17. **DerMardirossian C, Schnelzer A, Bokoch GM.** Phosphorylation of RhoGDI by Pak1 mediates dissociation of Rac GTPase. *Mol Cell* 15: 117–127, 2004.
18. **Dudek SM, Jacobson JR, Chiang ET, Birukov KG, Wang P, Zhan X, Garcia JG.** Pulmonary endothelial cell barrier enhancement by sphingosine 1-phosphate: roles for cactactin and myosin light chain kinase. *J Biol Chem* 279: 24692–24700, 2004.

19. Essler M, Amano M, Kruse HJ, Kaibuchi K, Weber PC, Aepfelbacher M. Thrombin inactivates myosin light chain phosphatase via Rho and its target Rho kinase in human endothelial cells. *J Biol Chem* 273: 21867–21874, 1998.
20. Gniwotta C, Morrow JD, Roberts LJ, 2nd, Kuhn H. Prostaglandin F<sub>2</sub>-like compounds, F<sub>2</sub>-isoprostanes, are present in increased amounts in human atherosclerotic lesions. *Arterioscler Thromb Vasc Biol* 17: 3236–3241, 1997.
21. Herbrand U, Ahmadian MR. p190-RhoGAP as an integral component of the Tiam1/Rac1-induced downregulation of Rho. *Biol Chem* 387: 311–317, 2006.
22. Hodge DR, Hurt EM, Farrar WL. The role of IL-6 and STAT3 in inflammation and cancer. *Eur J Cancer* 41: 2502–2512, 2005.
23. Holme PA, Solum NO, Brosstad F, Roger M, Abdelnoor M. Demonstration of platelet-derived microvesicles in blood from patients with activated coagulation and fibrinolysis using a filtration technique and western blotting. *Thromb Haemost* 72: 666–671, 1994.
24. Huber J, Vales A, Mitulovic G, Blumer M, Schmid R, Witztum JL, Binder BR, Leitinger N. Oxidized membrane vesicles and blebs from apoptotic cells contain biologically active oxidized phospholipids that induce monocyte-endothelial interactions. *Arterioscler Thromb Vasc Biol* 22: 101–107, 2002.
25. Jerlich A, Schaur RJ, Pitt AR, Spickett CM. The formation of phosphatidylcholine oxidation products by stimulated phagocytes. *Free Radic Res* 37: 645–653, 2003.
26. Jones SA, Richards PJ, Scheller J, Rose-John S. IL-6 transsignaling: the in vivo consequences. *J Interferon Cytokine Res* 25: 241–253, 2005.
27. Leitinger N. Oxidized phospholipids as triggers of inflammation in atherosclerosis. *Mol Nutr Food Res* 49: 1063–1071, 2005.
28. Leitinger N, Tyner TR, Oslund L, Rizza C, Subbanagounder G, Lee H, Shih PT, Mackman N, Tigyi G, Territo MC, Berliner JA, Vora DK. Structurally similar oxidized phospholipids differentially regulate endothelial binding of monocytes and neutrophils. *Proc Natl Acad Sci USA* 96: 12010–12015, 1999.
29. Li R, Mouillesseaux KP, Montoya D, Cruz D, Gharavi N, Dun M, Koroniak L, Berliner JA. Identification of prostaglandin E<sub>2</sub> receptor subtype 2 as a receptor activated by OxPAPC. *Circ Res* 98: 642–650, 2006.
30. Liu F, Verin AD, Borbiev T, Garcia JG. Role of cAMP-dependent protein kinase A activity in endothelial cell cytoskeleton rearrangement. *Am J Physiol Lung Cell Mol Physiol* 280: L1309–L1317, 2001.
31. Ma Z, Li J, Yang L, Mu Y, Xie W, Pitt B, Li S. Inhibition of LPS- and CpG DNA-induced TNF- $\alpha$  response by oxidized phospholipids. *Am J Physiol Lung Cell Mol Physiol* 286: L808–L816, 2004.
32. Mehta D, Malik AB. Signaling mechanisms regulating endothelial permeability. *Physiol Rev* 86: 279–367, 2006.
33. Moy ABBJE, Blackwell K, Shasby SS, Shasby DM. cAMP protects endothelial barrier function independent of inhibiting MLC20-dependent tension development. *Am J Physiol Lung Cell Mol Physiol* 274: L1024–L1029, 1998.
34. Nakamura T, Henson PM, Murphy RC. Occurrence of oxidized metabolites of arachidonic acid esterified to phospholipids in murine lung tissue. *Anal Biochem* 262: 23–32, 1998.
35. Nonas SA, Miller I, Kawkitinarong K, Chatchavalvanich S, Gorshkova I, Bochkov VN, Leitinger N, Natarajan V, Garcia JG, Birukov KG. Oxidized phospholipids reduce vascular leak and inflammation in rat model of acute lung injury. *Am J Respir Crit Care Med* 173: 1130–1138, 2006.
36. Noritake J, Watanabe T, Sato K, Wang S, Kaibuchi K. IQGAP1: a key regulator of adhesion and migration. *J Cell Sci* 118: 2085–2092, 2005.
37. Parker JC. Inhibitors of myosin light chain kinase and phosphodiesterase reduce ventilator-induced lung injury. *J Appl Physiol* 89: 2241–2248, 2000.
38. Peng X, Hassoun PM, Sammani S, McVerry BJ, Burne MJ, Rabb H, Pearse D, Tuder RM, Garcia JG. Protective effects of sphingosine 1-phosphate in murine endotoxin-induced inflammatory lung injury. *Am J Respir Crit Care Med* 169: 1245–1251, 2004.
39. Qiao J, Huang F, Lum H. PKA inhibits RhoA activation: a protection mechanism against endothelial barrier dysfunction. *Am J Physiol Lung Cell Mol Physiol* 284: L972–L980, 2003.
40. Shikata Y, Rios A, Kawkitinarong K, DePaola N, Garcia JG, Birukov KG. Differential effects of shear stress and cyclic stretch on focal adhesion remodeling, site-specific FAK phosphorylation, and small GTPases in human lung endothelial cells. *Exp Cell Res* 304: 40–49, 2005.
41. Tamma G, Klussmann E, Prociño G, Svelto M, Rosenthal W, Valenti G. cAMP-induced AQP2 translocation is associated with RhoA inhibition through RhoA phosphorylation and interaction with RhoGDI. *J Cell Sci* 116: 1519–1525, 2003.
42. Van Nieuw Amerongen GP, Natarajan K, Yin G, Hoefen RJ, Osawa M, Haendeler J, Ridley AJ, Fujiwara K, van Hinsbergh VW, Berk BC. GIT1 mediates thrombin signaling in endothelial cells: role in turnover of RhoA-type focal adhesions. *Circ Res* 94: 1041–1049, 2004.
43. Van Nieuw Amerongen GP, van Delft S, Vermeer MA, Collard JG, van Hinsbergh VW. Activation of RhoA by thrombin in endothelial hyperpermeability: role of Rho kinase and protein tyrosine kinases. *Circ Res* 87: 335–340, 2000.
44. Waddington EI, Puddey IB, Mori TA, Croft KD. Similarity in the distribution of F<sub>2</sub>-isoprostanes in the lipid subfractions of atherosclerotic plaque and in vitro oxidised low density lipoprotein. *Redox Rep* 7: 179–184, 2002.
45. Walton KA, Cole AL, Yeh M, Subbanagounder G, Krutzik SR, Modlin RL, Lucas RM, Nakai J, Smart EJ, Vora DK, Berliner JA. Specific phospholipid oxidation products inhibit ligand activation of toll-like receptors 4 and 2. *Arterioscler Thromb Vasc Biol* 23: 1197–1203, 2003.
46. Watson AD, Leitinger N, Navab M, Faull KF, Horkko S, Witztum JL, Palinski W, Schwenke D, Salomon RG, Sha W, Subbanagounder G, Fogelman AM, Berliner JA. Structural identification by mass spectrometry of oxidized phospholipids in minimally oxidized low density lipoprotein that induce monocyte/endothelial interactions and evidence for their presence in vivo. *J Biol Chem* 272: 13597–13607, 1997.
47. Watson AD, Subbanagounder G, Welsbie DS, Faull KF, Navab M, Jung ME, Fogelman AM, Berliner JA. Structural identification of a novel pro-inflammatory epoxyisoprostane phospholipid in mildly oxidized low density lipoprotein. *J Biol Chem* 274: 24787–24798, 1999.
48. Wood LG, Gibson PG, Garg ML. Biomarkers of lipid peroxidation, airway inflammation and asthma. *Eur Respir J* 21: 177–186, 2003.
49. Yeh M, Cole AL, Choi J, Liu Y, Tulchinsky D, Qiao JH, Fishbein MC, Dooley AN, Hovnanian T, Mouillesseaux K, Vora DK, Yang WP, Gargalovic P, Kirchgessner T, Shyy JY, Berliner JA. Role for sterol regulatory element-binding protein in activation of endothelial cells by phospholipid oxidation products. *Circ Res* 95: 780–788, 2004.
50. Zheng Y. Dbl family guanine nucleotide exchange factors. *Trends Biochem Sci* 26: 724–732, 2001.